Mon. Not. R. Astron. Soc. **000**, 1–7 () Printed 5 February 2008 (MN LATEX style file v2.2)

Galaxy morphologies and environment in the Abell 901/902 supercluster from COMBO-17

K. P. Lane[1⋆], M. E. Gray[1], A. Aragón-Salamanca[1], C. Wolf[2], K. Meisenheimer [3]
1. School of Physics and Astronomy, The University of Nottingham, University Park, Nottingham, NG7 2RD
2. Department of Physics, Denys Wilkinson Bldg., University of Oxford, Keble Road, Oxford OX1 3RH
3. Max-Planck-Institut für Astronomie, Königstuhl 17, D-69117, Heidelberg, Germany

ABSTRACT
We present a morphological study of galaxies in the A901/902 supercluster from the COMBO-17 survey. A total of 570 galaxies with photometric redshifts in the range $0.155 < z_{\rm phot} < 0.185$ are visually classified by three independent classifiers to $M_V = -18$. These morphological classifications are compared to local galaxy density, distance from the nearest cluster centre, local surface mass density from weak lensing, and photometric classification. At high local galaxy densities $\log \Sigma_{10}/\mathrm{Mpc}^2 > 1.5$ a classical morphology-density relation is found. A correlation is also found between morphology and local projected surface mass density, but no trend is observed with distance to the nearest cluster. This supports the finding that local environment is more important to galaxy morphology than global cluster properties. The breakdown of the morphological catalogue by colour shows a dominance of blue galaxies in the galaxies displaying late-type morphologies and a corresponding dominance of red galaxies in the early-type population. Using the 17-band photometry from COMBO-17, we further split the supercluster red sequence into old passive galaxies and galaxies with young stars and dust according to the prescription of Wolf et al. (2005). We find that the dusty star-forming population describes an intermediate morphological group between late-type and early-type galaxies, supporting the hypothesis that field and group spiral galaxies are transformed into S0s and, perhaps, ellipticals during cluster infall.

Key words: galaxies: clusters: general — galaxies: evolution — galaxies: interactions

1 INTRODUCTION

The precise role that environment plays in transforming the morphological and star-formation properties of galaxies as they are accreted onto groups and clusters remains unclear. Well-known correlations of cluster properties with environment hinting at evolutionary effects include the cluster morphology-density relation (Dressler 1980; Dressler et al. 1997) and the increasing fraction of blue galaxies in clusters at higher redshift (Butcher & Oemler 1978, 1984). A galaxy's encounters with other galaxies, with a hot intracluster medium (ICM) or with a tidal cluster potential could all be pathways to morphological alteration. However, it is also possible that galaxies in the densest regions formed earlier, evolved more quickly, and thus display more mature evolutionary states.

Dressler et al. (1997) find that at z $\sim$ 0.5 the fraction of S0s is significantly lower than at present, with a proportional increase in the spiral fraction. As the fraction of ellipticals is already similar to that found locally, it is surmised that the low-z S0 population formed chiefly from spirals. One way to investigate the effect of environment is to search for transitional objects in the process of transformation. For example, 'passive spirals' displaying spiral arms but no signatures of star formation could be identified as an intermediary stage between spirals and S0s (Goto et al. 2003; Poggianti 2004). It is therefore important to examine the variation of morphological populations with environment (local mass, gas, and galaxy densities) to determine the physical processes at work.

Historically both relaxed and irregular clusters have been the focus of morphological analysis. In fact Dressler (1980) showed that the morphology-density relation is present in both. This implies that morphological segregation is already in progress before cluster virialisation, if heirarchical models of structure formation are to be believed. An advanced stage of evolution will lead to cluster properties being strongly correlated, and corresponding signatures of different environmental influences may then be difficult to untangle. In order to decouple the effects of mass density, galaxy density, cluster-centric distance and gas content on galaxy morphologies it is necessary to examine systems still in the process of formation. In a system that has not yet reached equilibrium, the different components of the structure may still be segregated.

To this end we morphologically classify galaxies in the Abell 901(a,b)/902 supercluster, a structure consisting of three clusters and associated groups all within 5×5 Mpc at $z = 0.17$. We use imaging data from the COMBO-17 survey of this region (Wolf et al. 2001, 2004), which includes observations from the ESO/MPG

⋆ email: *ppxkl@nottingham.ac.uk*

Wide-Field Imager in broad-band $UBVRI$ and a further 12 medium-band optical filters. The 17-band photometry provides precision photometric redshifts (mean error $\sigma_z/(1+z) < 0.01$ for $R < 20$ galaxies) and spectral energy distributions (SEDs). Additionally, a deep R-band image ($R < 25.5$) with $0.7''$seeing provides excellent image quality for visual classifications and weak gravitational lensing. Further multiwavelength coverage from X-ray to MIR of the $0.5^\circ \times 0.5^\circ$ field includes observations with XMM-Newton, GALEX, Spitzer, a NIR extension to COMBO-17 using Omega2000 on Calar Alto, plus spectra of the 300 brightest cluster members from 2dF. This extensive data set makes the supercluster a uniquely well-positioned subject for detailed studies of galaxy evolution. The utility of this field will be greatly extended by a forthcoming HST mosaic as part of the STAGES survey.

Additional interest comes from the fact that the supercluster is dynamically complex, with no clear scaling relations between mass from weak lensing maps (Gray et al. 2002; Taylor et al. 2004), galaxy number density, velocity dispersion, and X-ray luminosity (Gray et al, in prep). This provides an excellent opportunity to investigate which environmental properties have the greatest influence on galaxy evolution, bearing in mind the important caveat that all such quantities are seen in projection. Here we investigate correlations of visually classified galaxy morphologies with environment. Throughout we use a concordance cosmology with $\Omega_m = 0.27$, $\Omega_\lambda = 0.73$, and $H_0 = 71$ km s^{-1} Mpc^{-1} so that 1 arcmin = 168 kpc at the redshift of the supercluster.

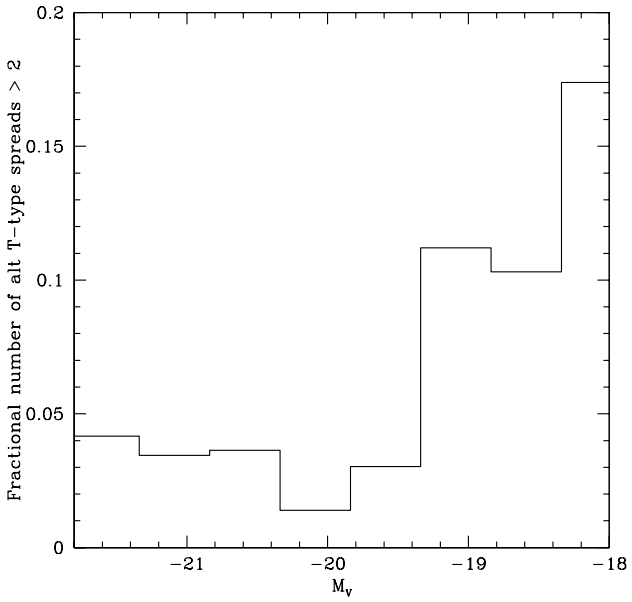

Figure 1. Effects of magnitude on classification precision. The fraction of galaxies with a spread in classification of > 2 alternative T-types from 3 independent classifiers is shown as a function of absolute magnitude. By $M_V = -18$ the fraction of galaxies with a spread in classifications > 2 is almost 20%.

2 VISUAL GALAXY CLASSIFICATION

The cluster sample was chosen by a $0.155 < z < 0.185$ cut in photometric redshift at an initial absolute magnitude cut of $M_V = -19$ (all magnitudes are Vega). According to Wolf et al. (2005), $\sigma_z < 0.01$ for this sample gives 99% completeness, if a Gaussian distribution is assumed. Using the same redshift range but increasing the magnitude depth to $M_V = -18$ increases the error in the photo-z to $\sigma \approx 0.015$ and therefore the completeness is $\sim 68\%$ at this luminosity limit. The above sample of cluster galaxies is estimated to have ~ 60 non-cluster contaminants (Wolf et al. 2005). This represents 8.6% of our sample and so only introduces small uncertainties into our results.

Classifications were performed independently by three of the authors (KPL, MEG, AAS) and combined in order to reduce classifier bias. Galaxies were classified according to de Vaucouleurs' T-type scheme, in which -5 is elliptical, -2 = S0, 1 = Sa, 2 = Sab, 3 = Sb, 4 = Sbc, 5 = Sc, 6 = Scd, 7 = Sd, 8 = Sdm, 9 = Sm/Irr (de Vaucouleurs 1959). However, in terms of real ability to discriminate by the classifiers this version of the T scale is distorted: for example, a gap of three between E and S0s is far too wide. We therefore adopted an alternative T-type scale where the difference between adjacent T-types is set to one and the gap between a given Hubble type and its intermediary (e.g. Sa/Sab) is taken as a difference of 0.5. Additionally, the scheme allows combined classifications in the case where a classifier cannot positively separate two adjacent T-types (the most common example being E/S0 or S0/E). The relative weighting assigned to the primary and secondary choices is discussed below. Comments were recorded if the morphology was abnormal in any way and galaxies were flagged if they showed visual signs of asymmetry, merger, or interaction.

Combining the three classification sets gives some measure of the reliability of the classifications. Fig. 1 shows the fraction of galaxies with a disagreement of more than two alternative T-types over the three independent classifications. The level of disagreement increases with greater magnitude as the galaxies become fainter and their structure harder to discern. Above an absolute magnitude of -18 the disagreement of > 2 alternative T-types reaches $\sim 20\%$ of galaxies. A magnitude limit of $M_V = -18$ was therefore adopted for further morphological analysis resulting in 570 galaxies.

These three classification sets were combined into one overall set according to a set of rules based on the prescription used by the EDisCS group (Desai et al. 2006). For each galaxy, the final classification was computed by an equally weighted combination of the three sets. In the case of a combined classification where a classifier was unable to discriminate between adjacent T-types, the primary and secondary classifications were assigned 3/4 and 1/4 of that classifier's weighting, respectively. The T-type with the highest combined weighting was taken as the final classification for that galaxy. If two T-types had equal combined weightings the final classification was randomly selected between them. Finally, in the case where there were more than two equally weighted types the differences between the types were computed. If one difference was $\leqslant 3$ on the alternative T-type scale the final classification was again chosen randomly between the two types spanning this gap. Otherwise if there was more than one gap of this size or none $\leqslant 3$ then the median of the equally highly-weighted T-types was taken as the final classification. The final Hubble type classification catalog was comprised of 275 ellipticals, 126 S0, 59 Sa, 15 Sab, 49 Sb, 8 Sbc, 9 Sc, 2 Scd, 19 Sm/Irr and 6 unknown galaxies. For use in the following morphology-environment studies spirals and Irr were binned together (167 in all), but given the small numbers it would make no difference if we considered only pure spirals.

The visual distinction between an S0 galaxy and an elliptical is difficult, especially if the S0 is face on. Following Dressler et al. (1997) we gauge the reliabilty of our S0/E separation by comparing the ellipticities of our classified galaxies to the ellipticities of

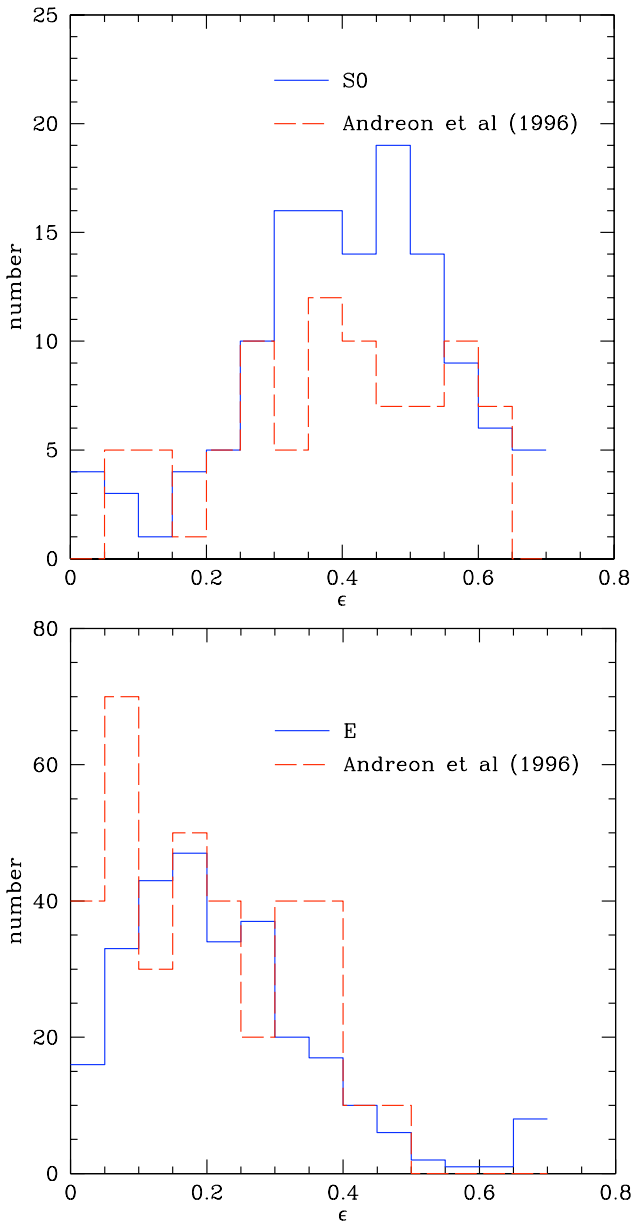

Figure 2. Comparison of the ellipticities of the samples classified as Ellipticals and S0s in the A901/2 field with the ellipticities of the corresponding morphological samples as found in the Coma cluster (Andreon et al. 1996). The good agreement between the distributions of ellipticities in our samples and those in the Coma cluster, combined with the different ellipticity distributions of our Elliptical and S0 samples, provides some confidence in our ability to separate Elliptical and S0 classes.

galaxies in the Coma cluster (Andreon et al. 1996, see Fig 2). Ellipticities were measured from the R-band image using SExtractor (Bertin & Arnouts 1996). Kolmogorov-Smirnov tests give confidence intervals of 98.9% for ellipticals and 53.1% for S0s being drawn from the same populations as their Andreon et al. (1996) counterparts. This compares with an $\sim 10^{-6}$ confidence that our ellipticals and S0s are drawn from the same population. These results provide some confidence that we have reliably separated these two classes.

3 LINKING MORPHOLOGY TO CLUSTER ENVIRONMENT

The morphology-density, or $\Sigma - T$, relation has been observed in a large range of galaxy environments, from rich cluster cores, groups, to field densities (e.g. Postman & Geller 1984; Treu et al. 2003). Several physical mechanisms may be responsible for transforming galaxy morphologies. These will be effective in different regimes: e.g. in groups where galaxy density increases over the field, but where relative velocities are still low, galaxy-galaxy interactions including major mergers may play a large role (Barnes 1992). The high velocities reached by galaxies in the cores of rich clusters make mergers less likely, but increase the efficacy of high-speed interactions such as harassment (Moore et al. 1999). Likewise, cluster-specific mechanisms such as tidal stripping (Merritt 1983) or the removal of a galaxy's hot (Larson et al. 1980) or cold (Gunn & Gott 1972) gas by ram-pressure processes require a steep potential or high ICM densities and so are more likely to take effect in the inner regions of clusters.

In light of the many physical mechanisms that may be at work in different regimes, we examine galaxy morphology as a function of several different proxies for 'environment': local galaxy density, projected mass density from lensing, and distance to the nearest cluster centre.

3.1 Linking morphology to local projected galaxy density

The projected local galaxy density, Σ_{10}, was found by calculating the area encompassed by the galaxy in question and its 9 nearest neighbours. Only galaxies to $M_V = -18$ were used when calculating Σ_{10} as fainter galaxies will decrease completeness.

Galaxies lying nearer to the edge of the image field than their 9th nearest neighbour were removed from the catalogue, 37 in all. This was to avoid anomalously low densities resulting from missing neighbouring galaxies outside the field-of-view.

Due to uncertainties in the photometric redshifts ($\sigma \approx 0.015$ at the magnitude limit used in this study, $M_V < -18$), we estimate that $\sim$ 95 potential field galaxies cannot be ruled out as cluster members. This implies the minimum density we can measure is $\sim$ 3.6Mpc^{-2}. However, this is much smaller than the lowest densities considered in our study ($\sim$ 25Mpc^{-2}).

The $\Sigma - T$ relation (Fig. 3) shows a strong increase in the fraction of ellipticals at high densities, a corresponding fall in the fraction of spirals and the S0 fractions show no correlation. This is the classical morphology-density relation as seen in numerous other studies (e.g. Oemler 1974; Dressler 1980; Dressler et al. 1997; Treu et al. 2003). Error bars are multinomial and were determined using Monte Carlo simulations.

By analysing data in the range $0 < z < 1$, including Dressler (1980) at $z \sim 0$ and Dressler et al. (1997) at $z \sim 0.5$, Smith et al. (2005) and Postman et al. (2005) find that the gradient of the early type $\Sigma - T$ relation increases with lowering z due to reducing numbers of spirals and increasing numbers of S0s, especially in high density regions. It is difficult to compare the results presented in Fig. 3 with these studies because they use depths comparable to that used by Dressler (1980). To enable a comparison we cut our sample to the same depth as used by Dressler (1980) ($M_V = -19.6$), after correcting for differences in the cosmology used. Doing so reduces the number of sources in our classified sample by more than a factor of 2 which increases the error bars to point where no trends can be seen. However it is noted that in our samples there are smaller fractions of S0s and larger fractions of Es when compared with

Dressler (1980). This could be due to cluster to cluster variation or systematic differences in classification.

If we compare our full sample with that of Dressler (1980) relative to the cluster core Σ_{10}, the gradient in the $\Sigma - T$ relation for our elliptical population is shallower than found in the highest density regions by Dressler (1980). There are also smaller fractions of S0s and larger fractions of spirals as compared with Dressler (1980). This is in agreement with the findings of Smith et al. (2005) and Postman et al. (2005). At lower densities we find larger fractions of ellipticals than Dressler (1980). That our fractions of S0s are so much smaller than Dressler (1980), and that our elliptical fractions are so much larger, is unexpected. However, S0 fraction does vary by large amounts from cluster to cluster and the criteria used to separate E and S0 classes varies from study to study. We also note that the fraction of early types (elliptical + S0) in our highest density bins is in keeping with the positive trend found in the fraction of early type galaxies with decreasing redshift in high density regions (Smith et al. 2005). Again it is noted that this comparison is made using our full sample to $M_V = -18$ to enable sample errors to be reduced to the point where trends can be seen.

With the adopted cosmology, 1 arcsecond corresponds to 2.80kpc at the cluster redshift. Similarly the seeing limited resolution of our image is 1.96kpc at the cluster redshift. This compares with $\sim$ 700pc for Postman et al. (2005), using HST ACS data, at $z \sim 1$, and $\sim$ 500pc for Dressler et al. (1997), using HST WFPC2 data, at $z \sim 0.5$. Our resolution may result in later type spirals being classified as earlier types since fine structure will be harder to discern. This situation will be improved by using HST ACS data obtained as part of the STAGES project.

Fasano et al. (2000) use ground based data with resolution 2-4 kpc at the redshifts of their clusters ($0.1 \lesssim z \lesssim 0.25$). Again no comparisons can be drawn when our sample is cut to the same absolute magnitude ($M_V = -20$). However, when comparing our full sample we find good agreement between our MD relation and the MD relation found by Fasano et al. (2000) in their high elliptical-concentration clusters. Our data fits the trend of rising S0 fraction, falling Sp fraction and no evolution in the fraction of E with redshift. We also find our data to be consistent with the rising trends in the N_{S0}/N_E and N_{S0}/N_{sp} fractions with lowering redshift, as presented in Fasano et al. (2000).

Note that the dynamic range in our Σ_{10} measurements is somewhat smaller than in the above studies, particularly at low densities. However, this does not have a significant effect on the comparisons discussed above.

3.2 Linking morphology to projected cluster mass

As the mass of a cluster is made up predominantly of dark matter, one might expect various environmental properties, such as local galaxy density and the intracluster medium (ICM), to trace the potential wells described by the dark matter mass of the cluster. This may well be true in a virialised cluster where there is a positional degeneracy between such environmental factors, however maps of projected mass and galaxy distribution (Gray et al. 2002) and extended X-ray emission (Gray et al, in prep) show that in the A901/902 supercluster such scaling relations are not self-consistent from cluster to cluster. For example, Abell 901b displays a prominent mass peak and $L_X = 2.35 \times 10^{44}$ erg s^{-1}, yet is relatively deficient in galaxy numbers. This then provides an opportunity to ascertain if cluster mass has a direct effect on galaxy morphology, or whether it is merely a tracer of other morphology affecting environmental properties.

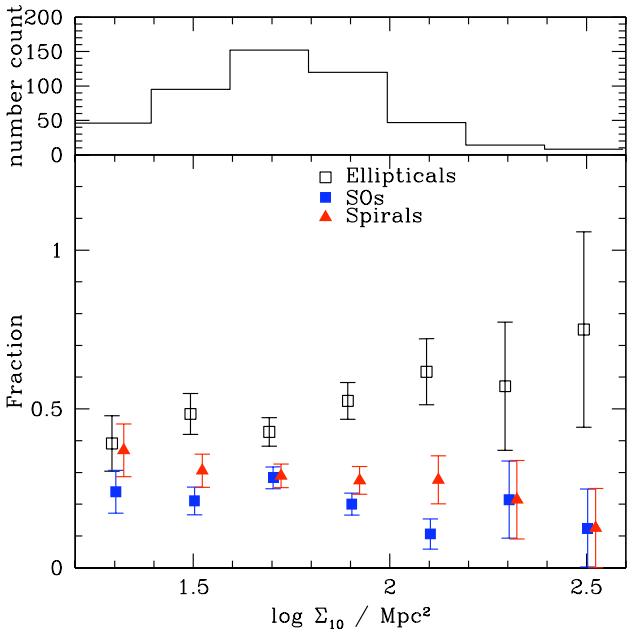

Figure 3. Morphological type, as a fraction of the total, with increasing local density. At high density there is a clear upward trend in ellipticals and a downward trend in spirals. There appears to be no trend in S0s. We ignored bins with fewer than 5 galaxies due to the large sampling errors. This corresponds to log $\Sigma_{10} < 1.3$. The upper panel shows the total number of galaxies in each density bin.

The projected surface mass density for this region was reconstructed by Gray et al. (2002) from an analysis of weak lensing of faint galaxies in the same COMBO-17 image. The surface mass is measured as a dimensionless quantity κ, where $\kappa = \Sigma/\Sigma_{\rm crit}$ is the ratio of the projected surface mass density to the critical surface mass density for lensing for a fixed source and lens redshift. For the supercluster lens at $z = 0.17$ and a population of faint lensed galaxies with $\langle z \rangle \sim 1$ we have $\Sigma_{\rm crit} = 5.0 \times 10^{15} h M_{\odot}$ Mpc^{-2}. The Gray et al. (2002) map includes smoothing with a Gaussian of $\sigma = 60$ arcsec, and the rms noise in the map was estimated as $\sigma_\kappa = 0.027$ through simulations.

Fig. 4 shows a clear relation between projected mass and morphology (a $\kappa - T$ relation) similar to the observed $\Sigma - T$ relation, but only at high mass densities (corresponding to the 3σ κ error regime). An upward trend with κ is found in ellipticals and a downward trend in S0s, however spirals do not show any correlation with projected mass. The different trends observed between Σ_{10} and κ suggest that both are tracers of morphology. Whether they are indepenent or, as is more likely, they are tracers of different aspects of the same environmental driver for morphology, remains to be determined. Fewer than 30% of galaxies in the highest κ bins are classified as spirals. This is analogous to the star-formation–κ relation found for the supercluster by Gray et al. (2004), where the highest density regions were found to be populated almost exclusively by galaxies with quiescent SEDs.

3.3 Linking morphology to cluster radius

Any correlation between clustercentric radius and the morphology of a galaxy ($R - T$ relation) will most likely be a reflection of global rather than local properties of the cluster since radius is not a localised quantity.

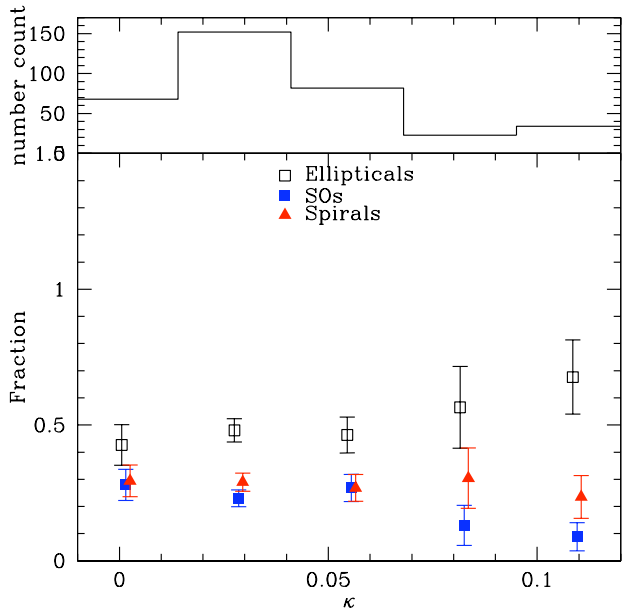

Figure 4. Morphological type, as a fraction of the total, with increasing projected surface mass density, κ, from lensing. At high surface density an upward trend in ellipticals and a downward trend in S0s is observed. No clear trend is found in the spiral population. The upper panel shows the total number of galaxies in each κ bin. The bin width corresponds to the noise of the κ maps, $\sigma_\kappa = 0.027$.

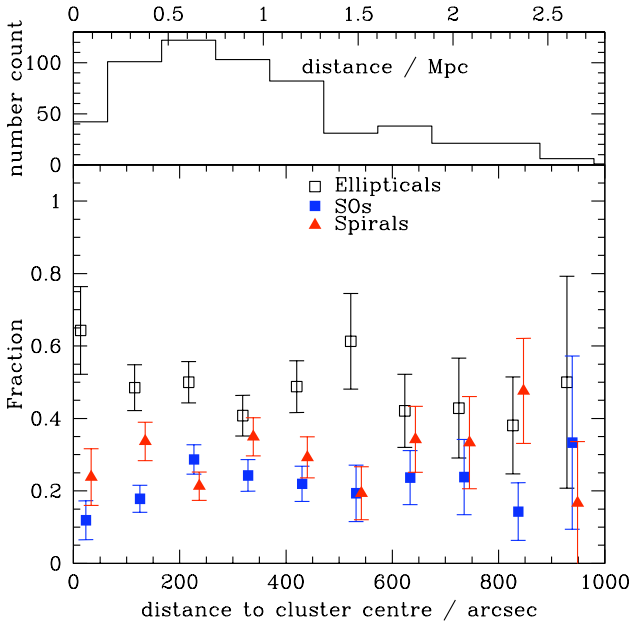

Figure 5. Morphological type, as a fraction of the total, with increasing distance to nearest cluster centre. No clear trend is observed with increasing radial distance. Data points with zero sample size have undetermined errors.

The clustercentric radius is the distance to the nearest cluster, where the cluster centre was defined as the peak of the κ map, although BCGs could have been used without much change. Fig. 5 shows that there is no clear trend between galaxy morphology and cluster radius, with only a small rise in elliptical fractions and a small decrease in late-type and S0 fractions at small radii. These small radii correspond to regions which would be the least affected by the large scale cluster merger. This result may then reflect the virialized cluster cores where radius is degenerate with projected mass.

The presence of a relation between morphology and local galaxy density, combined with this apparent lack of a relation between morphology and clustercentric radius adds further weight to the hypothesis that local conditions have more effect on galaxy morphology than global cluster properties. Previous studies (Dressler et al. 1997) have shown that any radial dependence of morphology is most likely a reflection of the $\Sigma - T$ relation due to the one-to-one correspondence between density and radius in relaxed clusters. For the A901/902 system in particular the cluster properties and radius are more decoupled than in relaxed systems due to the dynamical complexity. However, one caveat relevant to both the $\Sigma - T$ and $R - T$ correlations is the possibility of projection effects, particularly in the region between the A901a and A901b clusters. This possibility has been checked by masking out this region and is found to have no appreciable effect on the above results and hence is ruled out as a source of uncertainty.

4 LINKING MORPHOLOGY TO PHOTOMETRIC CLASSIFICATION

In Wolf et al. (2005) the Abell 901/902 cluster galaxy sample examined here was divided into three subpopulations: red, passively evolving galaxies; blue star-forming galaxies; and a previously unknown third population of red galaxies revealed by the 17-band photometry. This third population consists of cluster galaxies also located along the cluster red sequence, but containing significant amounts of young stars and dust (hereafter referred to as 'dusty red galaxies').

Examining the photometric class of each morphological type, Fig. 6 shows a clear trend. The majority of morphologically early-type galaxies (E,S0) are photometrically passive and red. Late-type galaxies (Sb,Sc) are predominantly blue. The third population of dusty red galaxies, on the other hand, shows a distinct distribution of intermediate morphologies. In this case intermediate types have been binned with the next highest integer alternative T-type for clarity, e.g. Sab is binned with Sb, Sbc with Sc and so on.

Two possible origins for this intermediate population of dusty red galaxies are posed by Wolf et al. (2005). Firstly, that they originate in the blue cloud and are in a state of being transformed into red cluster galaxies or, secondly, that they are the result of minor mergers of infalling galaxies with established cluster galaxies. To try and distinguish between these two formation scenarios the merger or interaction state of each galaxy was noted.

Of the classified galaxies which are photometrically found to be dusty and red, only $14.2\pm9.4\%$ were found by at least one classifier to be in a state of interaction with a neighbouring galaxy or undergoing a merger. This compares to $10.6\pm6.5\%$ of the classified passive red galaxies and $27.5\pm8.5\%$ of the classified blue galaxies. Within the uncertainties the three groups have consistent merger/interaction fractions, however, the low fraction of interactions/mergers for dusty red galaxies is inconsistent with a minor merger scenario for their formation. However, it should be noted that a large fraction of mergers may go undetected by a visual morphological analysis since this technique is only sensitive to asymmetries or tidal features in morphology which may not be present in a minor merger at scales larger than our resolution ($\sim$ 2 kpc).

Therefore the minor merger scenario for formation of dusty red galaxies cannot be ruled out, but does look unlikely.

The dusty red galaxies represent a significant proportion of the overall galaxy population (22.4%) and do not appear to be a subset of the blue or passive red galaxy populations. The differences in morphology are paralleled by differences in average spectra and spatial distributions shown in Wolf et al. (2005). In particular, they occupy regions of medium densities, avoiding high densities nearer the cluster core as well as low density regions in the cluster periphery (Wolf et al. 2005).

These pieces of evidence would then suggest that one major route in which infalling galaxies can be incorporated into the cluster is via transformative processes that do not necessarily involve mergers. Galaxies entering the cluster may have their star-formation ultimately quenched, but after an initial phase of enhanced star-formation (Milvang-Jensen et al. 2003; Bamford et al. 2005). A triggered starburst, possibly via interaction with the ICM, would introduce dust via supernovae feedback to produce the transitional dusty, red phase. Ultimately the gas supply will be exhausted and star formation quenched, leaving the remaining stars to evolve passively on the red sequence.

Dressler et al. (1999) and Poggianti et al. (1999) find similar spectroscopic populations of dusty starburst galaxies, or e(a) galaxies, at $z \sim 0.4 - 0.5$. They attribute these to the progenitors of post-starburst k+a/a+k galaxies. For the COMBO-17 A901/2 field spectra have been obtained for 64 cluster galaxies using the 2dF instrument (see Wolf et al. 2005). The average spectra for dusty red galaxies is seen to be inconsistent with that of k+a galaxies. The weak [OII] emission as well as Hδ absorption observed in the average spectra of these dusty red galaxies are consistent with e(a) type galaxies. To find such a large fraction (22.4%) of potential k+a progenitor galaxies at $z \sim 0.17$ is surprising given that Dressler et al. (1999) find that 18% of their cluster sample exhibit k+a/a+k spectral types at $z \sim 0.5$. However, the continuing cluster-cluster merger seen in the A901/2 system could well produce an increased incidence of e(a) galaxies due to the large number of infalling galaxies.

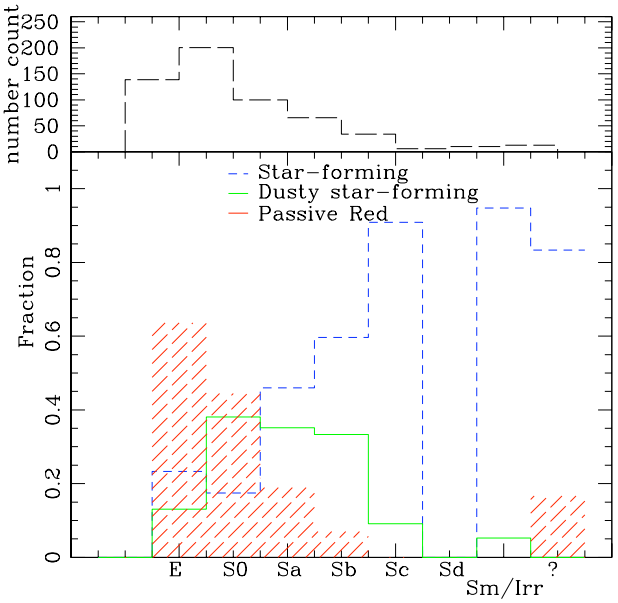

Figure 6. The photometric colour of each morphological type as a fraction of the total type population. Dusty red galaxies appear to form an intermediate regime between star-forming late-type galaxies and early-type passive galaxies. Data points with very large sampling error have been omitted.

5 CONCLUSIONS

The complex dynamics present in the Abell 901/902 systems provide an ideal testing ground for the distinction between the local and global processes driving galaxy morphology. In this paper we have examined relations between visual galaxy morphologies and local measures of environment including galaxy density, projected surface mass density from lensing, and clustercentric radius. The presence of a strong $\Sigma - T$ and $\kappa - T$ relations and absence of a corresponding $\Sigma - R$ relation shows that despite the large scale complexities of the clusters, local conditions are still well correlated to morphology.

Furthermore, the photometric breakdown of morphologies provides a tantalising glimpse of galaxy transformation during infall, in action. By determining the interaction and merger state of each classified galaxy it was shown that the population of red sequence galaxies with young stars and dust of Wolf et al. (2005) is not likely to be explained by minor mergers of infalling galaxies with cluster members. It is more plausible then that the dusty red galaxies are experiencing additional, cluster-specific phenomena during infall, causing their star-formation to become dust obscured and reddened. This would then support a picture of cluster formation in which accreted galaxies can be transformed through processes other than major or minor mergers, most likely through induced star-bursts and associated dust obscuration before the gas supply is stripped and/or exhausted, and star-formation stops.

This study will be extended in the forthcoming STAGES survey of the A901/902 supercluster. The survey consists of an 80 orbit mosaic using HST/ACS of the 0.5×0.5 degree region and will be combined with the 17-band photometric redshifts and other detailed multiwavelength data sets. This mosaic will be used for morphological classifications not only for the bright end of the cluster luminosity function probed here, but also the dwarf galaxy population, which may be more sensitive to environmental processes due to their lower gravitational potentials. In this way we will build up an even more detailed picture of galaxy evolution within a complex environment.

ACKNOWLEDGMENTS

KPL was supported by a PPARC studentship. MEG was supported by an Anne McLaren Research Fellowship from the University of Nottingham. C. Wolf was supported by a PPARC Advanced fellowship. Thanks go M. Merrifield and O. Almaini for useful and informative discussions. We thank the anonymous referee for comments which greatly improved the reliability of the results presented.

REFERENCES

Andreon S., Davoust E., Michard R., Nieto J.-L., Poulain P., 1996, A&A Supp., 116, 429
Bamford S. P., Milvang-Jensen B., Aragón-Salamanca A., Simard L., 2005, MNRAS, 361, 109
Barnes J. E., 1992, ApJ, 393, 484
Bertin E., Arnouts S., 1996, A&A Supp., 117, 393
Butcher H., Oemler A., 1978, ApJ, 226, 559

Butcher H., Oemler A., 1984, ApJ, 285, 426
de Vaucouleurs G., 1959, Handbuch der Physik, 53, 275
Desai V., Dalcanton J. J., Aragón-Salamanca A., Jablonka P., Poggianti B., Gogarten S. M., Simard L., Clowe D., Halliday C., Milvang-Jensen B., Pelló R., 2006, ApJ, p. submitted 2006
Dressler A., 1980, ApJ, 236, 351
Dressler A., Oemler A. J., Couch W. J., Smail I., Ellis R. S., Barger A., Butcher H., Poggianti B. M., Sharples R. M., 1997, ApJ, 490, 577
Dressler A., Smail I., Poggianti B. M., Butcher H., Couch W. J., Ellis R. S., Oemler A. J., 1999, ApJS, 122, 51
Fasano G., Poggianti B. M., Couch W. J., Bettoni D., Kjærgaard P., Moles M., 2000, ApJ, 542, 673
Goto T., Okamura S., Sekiguchi M., Bernardi M., Brinkmann J., Gómez P. L., Harvanek M., Kleinman S. J., Krzesinski J., Long D., Loveday J., Miller C. J., Neilsen E. H., Newman P. R., Nitta A., Sheth R. K., Snedden S. A., Yamauchi C., 2003, PASJ, 55, 757
Gray M. E., 2007, in prep
Gray M. E., Taylor A. N., Meisenheimer K., Dye S., Wolf C., Thommes E., 2002, ApJ, 568, 141
Gray M. E., Wolf C., Meisenheimer K., Taylor A., Dye S., Borch A., Kleinheinrich M., 2004, MNRAS, 347, L73
Gunn J. E., Gott J. R. I., 1972, ApJ, 176, 1
Larson R. B., Tinsley B. M., Caldwell C. N., 1980, ApJ, 237, 692
Merritt D., 1983, ApJ, 264, 24
Milvang-Jensen B., Aragón-Salamanca A., Hau G. K. T., Jørgensen I., Hjorth J., 2003, MNRAS, 339, L1
Moore B., Lake G., Quinn T., Stadel J., 1999, MNRAS, 304, 465
Oemler A. J., 1974, ApJ, 194, 1
Poggianti B., 2004, in Baryons in Dark Matter Halos Evolution of galaxies in clusters
Poggianti B. M., Smail I., Dressler A., Couch W. J., Barger A. J., Butcher H., Ellis R. S., Oemler A. J., 1999, ApJ, 518, 576
Postman M., Franx M., Cross N. J. G., Holden B., Ford H. C., Illingworth G. D., Goto T., others 2005, ApJ, 623, 721
Postman M., Geller M. J., 1984, ApJ, 281, 95
Smith G. P., Treu T., Ellis R. S., Moran S. M., Dressler A., 2005, ApJ, 620, 78
Taylor A. N., Bacon D. J., Gray M. E., Wolf C., Meisenheimer K., Dye S., Borch A., Kleinheinrich M., Kovacs Z., Wisotzki L., 2004, MNRAS, 353, 1176
Treu T., Ellis R. S., Kneib J., Dressler A., Smail I., Czoske O., Oemler A., Natarajan P., 2003, ApJ, in press (astro-ph/0303267)
Wolf C., Dye S., Kleinheinrich M., Meisenheimer K., Rix H.-W., Wisotzki L., 2001, A&A, 377, 442
Wolf C., Gray M. E., Meisenheimer K., 2005, A&A, 443, 435
Wolf C., Meisenheimer K., Kleinheinrich M., Borch A., Dye S., Gray M., Wisotzki L., Bell E. F., Rix H.-W., Cimatti A., Hasinger G., Szokoly G., 2004, A&A, 421, 913